THE JOURNAL OF PHYSICAL CHEMISTRY A
A JOURNAL OF THE AMERICAN CHEMICAL SOCIETY

pubs.acs.org/JPCA

Article

# Charge and Solvent Effects on the Redox Behavior of Vanadyl Salen−Crown Complexes

*Published as part of The Journal of Physical Chemistry virtual special issue "Steven G. Boxer Festschrift".*

Hien M. Nguyen, Harry W. T. Morgan, Teera Chantarojsiri, Tyler A. Kerr, Jenny Y. Yang, Anastassia N. Alexandrova,* and Nadia G. Léonard*

Cite This: *J. Phys. Chem. A* 2023, 127, 5324−5334

Read Online

ACCESS | Metrics & More | Article Recommendations | Supporting Information

**ABSTRACT:** The incorporation of charged groups proximal to a redox active transition metal center can impact the local electric field, altering redox behavior and enhancing catalysis. Vanadyl salen (salen = *N*,*N*′-ethylenebis(salicylideneaminato)) complexes functionalized with a crown ether containing a nonredox active metal cation (V-Na, V-K, V-Ba, V-La, V-Ce, and V-Nd) were synthesized. The electrochemical behavior of this series of complexes was investigated by cyclic voltammetry in solvents with varying polarity and dielectric constant ($\varepsilon$) (acetonitrile, $\varepsilon$ = 37.5; *N*,*N*-dimethylformamide, $\varepsilon$ = 36.7; and dichloromethane, $\varepsilon$ = 8.93). The vanadium(V/IV) reduction potential shifted anodically with increasing cation charge compared to a complex lacking a proximal cation ($\Delta E_{1/2}$ > 900 mV in acetonitrile and >700 mV in dichloromethane). In contrast, the reduction potential for all vanadyl salen−crown complexes measured in *N*,*N*-dimethylformamide was insensitive to the magnitude of the cationic charge, regardless of the electrolyte or counteranion used. Titration studies of *N*,*N*-dimethylformamide into acetonitrile resulted in cathodic shifting of the vanadium(V/IV) reduction potential with increasing concentration of *N*,*N*-dimethylformamide. Binding constants of *N*,*N*-dimethylformamide ($\log(K_{DMF})$) for the series of crown complexes show increased binding affinity in the order of V-La > V-Ba > V-K > (salen)V(O), indicating an enhancement of Lewis acid/base interaction with increasing cationic charge. The redox behavior of (salen)V(O) and (salen-OMe)V(O) (salen-OMe = *N*,*N*′-ethylenebis(3-methoxysalicylideneamine) was also investigated and compared to the crown-containing complexes. For (salen-OMe)V(O), a weak association of triflate salt at the vanadium(IV) oxidation state was observed through cyclic voltammetry titration experiments, and cation dissociation upon oxidation to vanadium(V) was identified. These studies demonstrate the noninnocent role of solvent coordination and cation/anion effects on redox behavior and, by extension, the local electric field.

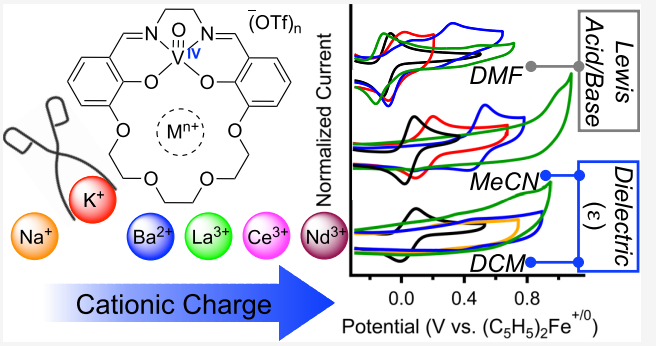




## I. INTRODUCTION

High-oxidation state vanadium (IV and V) complexes are often investigated for their reactivity in a variety of oxidation reactions.[1−3] Vanadyl complexes possess a vanadium−oxygen multiple bond and dominate the chemistry of vanadium due to their stability and have been used in many applications ranging from catalysis,[4−14] electrochemistry,[15,16] bioinorganic chemistry,[17−22] and molecular magnetism.[23−29] Specifically, salen (salen = *N*,*N*′-ethylenebis(salicylideneaminato)) vanadyl complexes have shown activity for the oxygen reduction reaction (ORR)[30] and autoxidation of alkenes.[31] Given the rich oxidation chemistry of vanadyl salen complexes, tuning their electrochemistry and redox behavior is useful for controlling their oxidation reactivity. Further, it is important to understand solvent effects on the redox properties, as it may determine reactivity profiles and stability of the vanadyl ion. Proximal nonredox active Lewis acidic metals are known to shift redox potentials and enhance reactivity.[32−45] Increasing the magnitude of charge of a positively charged ion or substituent typically results in an anodic shift (positive shift) of reduction potential. Investigations on charge effects on homogeneous transition metal complexes are important for understanding electron transfer processes, spectroscopic properties, and impact on catalytic activity.[46−48] Given the reversibility of the vanadyl (V/IV) redox couple and its role in reactions involving vanadium salen complexes, we investigated vanadyl salen-crown complexes containing various nonredox active

**Received:** February 6, 2023
**Revised:** May 29, 2023
**Published:** June 14, 2023

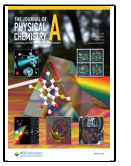

cations to modify the redox properties (Chart 1). Solvents with varying polarity and dielectric constant ($\varepsilon$) (acetonitrile, $\varepsilon$ = 37.5; *N*,*N*-dimethylformamide, $\varepsilon$ = 36.7; and dichloromethane, $\varepsilon$ = 8.93) were investigated to explore how both charge and solvent affect electron transfer, reorganization, and coordination around the vanadyl center. An understanding of the interplay of charge effects, solvent interactions, and redox behavior at vanadyl complexes informs how these characteristics influence reactivity.

**Chart 1. Vanadyl Complexes Investigated in This Study**

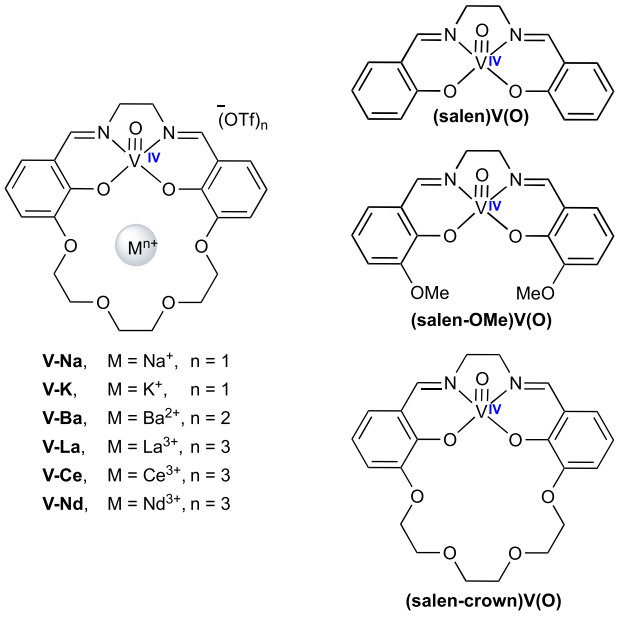


**V-Na**, M = $Na^+$, n = 1
**V-K**, M = $K^+$, n = 1
**V-Ba**, M = $Ba^{2+}$, n = 2
**V-La**, M = $La^{3+}$, n = 3
**V-Ce**, M = $Ce^{3+}$, n = 3
**V-Nd**, M = $Nd^{3+}$, n = 3

## II. EXPERIMENTAL METHODS

Reported salen-crown[49] and salen-crown-M[35,37,38,50] (M = $Na^+$, $K^+$, $Ba^{2+}$) were synthesized according to previously reported procedures. The vanadyl complexes were synthesized according to the procedures given in the SI. Vanadium(III) acetylacetonate ($V(acac)_3$), vanadyl acetylacetonate ($V(O)(acac)_2$), and triflate salts were purchased from Sigma-Aldrich and used as received. All nondeuterated solvents were degassed by sparging with argon and then dried by passage through an alumina column under argon pressure on a Solvent Drying System (JC Meyer Solvent Systems) and stored over activated 3 Å molecular sieves. Deuterated solvents were purchased from Cambridge Isotope Laboratories and used as received. NMR measurements were carried out at 298 K unless otherwise noted a Bruker DRX500 or AVANCE600 spectrometer. All $^1H$ and $^{13}C$ NMR chemical shifts are reported in ppm relative to $SiMe_4$ using $^1H$ (acetonitrile-$d_3$: 1.94 ppm, dichloromethane-$d_2$: 5.32 ppm) and $^{13}C$ (acetonitrile-$d_3$: 118.26, 1.32 ppm) chemical shifts of the solvent as a standard. High-resolution mass spectra (HRMS) were recorded on Waters LCT Premier TOF spectrometer with ESI and CI sources and collected at the University of California, Irvine Mass Spectrometry Facility. Elemental analyses were performed at UCI in the UC Irvine Materials Research Institute (IMRI) on a Thermo Scientific FlashSmart CHNS/O elemental analyzer. Continuous wave EPR spectra were recorded on an X-band Bruker EMX spectrometer equipped with an EMX standard resonator and a Bruker PremiumX microwave bridge. EPR spectra were collected as frozen solutions. The spectra were simulated using EasySpin[51] and Simultispin[52] for MATLAB.

**Electrochemical Analysis.** Cyclic voltammetry experiments were performed in an $N_2$-atmosphere glovebox using a Pine Wavedriver 10 potentiostat with AfterMath software, using a 1 mm diameter glassy carbon disc working electrode and glassy carbon rod counter electrode. Tetrabutylammonium hexafluorophosphate ($TBAPF_6$) was recrystallized from ethanol three times prior to use and was used as electrolyte unless otherwise noted. Cyclic voltammograms were measured for vanadium complexes in acetonitrile (MeCN), dimethylformamide (DMF), and dichloromethane (DCM) to investigate the impact of solvent on their electrochemical behavior. Solutions were prepared with 0.1 M $TBAPF_6$ electrolyte and 5 mM analyte. Ferrocene ($(C_5H_5)_2Fe$) or decamethylferrocene ($((CH_3)_5C_5)_2Fe$) was used to reference each individual spectrum. A $Ag/Ag^+$ pseudoreference electrode containing a silver wire submerged in 0.2 M solution of selected electrolyte separated from the bulk solution by a Vycor tip was used in addition to an internal ferrocene reference. Scans included IR drop compensation and ferrocene ($(C_5H_5)_2Fe$) or decamethylferrocene ($((CH_3)_5C_5)_2Fe$) was added as an internal reference for all experiments and each CV was carefully referenced individually. All redox potentials are reported versus $(C_5H_5)_2Fe^{+/0}$. When decamethylferrocene was used as an internal reference, redox potentials were corrected versus $(C_5H_5)_2Fe^{+/0}$ using reported values in the appropriate solvent.[53]

**Ultraviolet−Visible and Infrared Spectroscopies.** Ultraviolet−visible (UV−vis) spectra were collected in a 10 mm or 1 mm path length quartz cuvette, using Agilent Technologies Cary 60 UV−vis spectrometer. UV−vis spectroelectrochemistry experiments were conducted in a commercially available UV−vis spectroelectrochemistry kit from Pine Instrument with Pt working/counter electrode and Ag wire pseudo reference electrode. Stock solutions of vanadium(IV) oxido complexes (0.025 M) were prepared in MeCN or DMF for spectroelectrochemical studies. In a typical experiment, 0.3 mL of a 0.2 M solution of $TBAPF_6$ was placed in the spectroelectrochemical UV−vis cuvette (1 mm path length). A blank CV scan was then collected to ensure no redox features were observed prior to addition of the vanadium analyte. The vanadium(IV) oxido was then added to the cuvette by microsyringe (40 $\mu$L) to give a dilute solution of 0.3 mM. An initial UV−vis spectrum was then collected before a cyclic voltammogram was measured. The solution was then electrolyzed at 200 mV positive of the anodic peak corresponding to oxidation to the vanadium(V) oxido while UV−vis spectra were collected at 1 s increments until spectral changes were no longer observed. Infrared (IR) absorption measurements were taken as compressed solids or in solution where noted on a Thermo Scientific Nicolet iS5 spectrophotometer with an iD5 ATR attachment.

**X-ray Crystallography.** X-ray diffraction studies were carried out at the UCI Department of Chemistry, X-ray Crystallography Facility, on a Bruker SMART APEX II diffractometer. Data for V-Na, V-K, V-La, and V-Nd were collected at 93 K, and data for V-Ce and V-Ba were collected at 133 K. Data for V-Na, V-K, V-Ce, V-La, and V-Ba were collected using Mo K$\alpha$ radiation ($\lambda$ = 0.71073 Å) on a three-axis goniometer. Data for V-Nd were collected using Cu K$\alpha$ radiation ($\lambda$ = 1.54178 Å) on a three-axis goniometer. The APEX2 or APEX3 program suite was used to determine unit-


https://doi.org/10.1021/acs.jpca.3c00827
J. Phys. Chem. A 2023, 127, 5324−5334

**Scheme 1. Synthesis of Vanadyl Complexes**

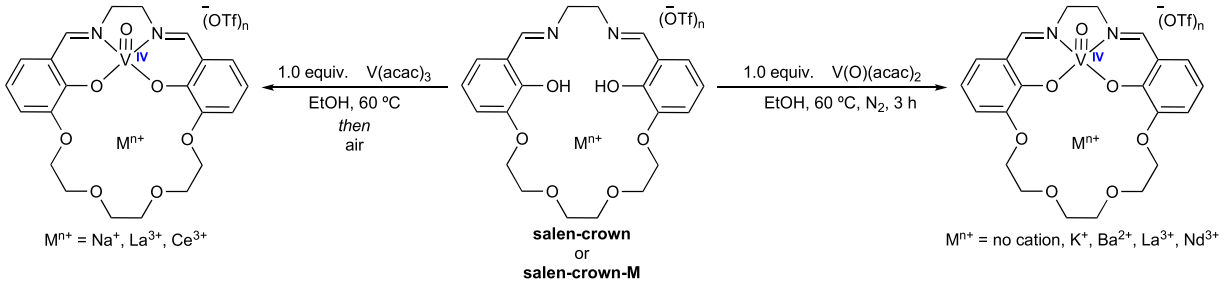


cell parameters and to collect data. The raw frame data were processed and absorption corrected using SAINT and SADABS (V-Na, V-K, V-La, V-Nd, V-Ba) or TWINABS (V-Ce) programs, respectively, to yield the reflection data files.[54,55] Structures were solved by direct methods using SHELXT and refined against $F^2$ on all data by full-matrix least-squares with SHELXL with SHELXle as GUI.[56−58] Twinned structure V-Nd was solved and refined as a pseudomerohedral twin on HKLF4 data; twinned structure V-Ce was solved on HKLF4 data and refined as a nonmerohedral twin on HKLF5 data. All nonhydrogen atoms were refined anisotropically with no constraints and few constraints on disordered parts. Hydrogen atoms were refined using a riding model, and their isotropic displacement parameters were fixed at 1.2 (1.5 for methyl groups) times the Ueq of the atoms to which they are bonded.

**Computational Methods.** DFT calculations were performed using ORCA[59] 5.0.2 using the wB97x-D3 functional.[60] The def2-TZVP basis set was used for all elements except C and H, for which def2-SVP was used.[61] All geometries were optimized for calculations of redox potentials.

## III. RESULTS AND DISCUSSION

**Synthesis and Structural Characterization.** Salen-crown-Ln ligands (Ln = $La^{3+}$, $Ce^{3+}$, $Nd^{3+}$) were prepared through metalation of salen-crown with the respective $Ln(OTf)_3$ salt in a 1:1 mixture of chloroform and methanol. The corresponding vanadyl complexes, V-M (M = $Na^+$, $K^+$, $Ba^{2+}$, $Nd^{3+}$, $La^{3+}$), were then isolated following metalation of the desired salen-crown-M ligand with $V(acac)_3$ (acac = acetylacetonate) in ethanol followed by exposure to air. Alternatively, the desired vanadyl complexes could be obtained directly through metalation of the salen-crown-M ligand with vanadyl acetylacetonate ($V(O)(acac)_2$) (Scheme 1). Single crystals suitable for X-ray diffraction of the vanadyl complexes (V-Na, V-K, V-Ba, V-La, V-Ce, V-Nd) were obtained following slow diffusion of diethyl ether into concentrated acetonitrile solutions at room temperature (Figure 1). Attempts to obtain X-ray quality crystals of the empty crown vanadyl complex ((salen-crown)V(O)) through slow diffusion of diethyl ether into either acetonitrile or *N*,*N*-dimethylforamide solutions were unsuccessful. Complexes (salen)V(O) and (salen-OMe)-V(O) were prepared according to previously reported procedures.[62]

In the solid state, V-Na and V-Ba complexes exist as dimers where the oxo ligand bridges between the vanadium and cation, M (M = $Na^+$ or $Ba^{2+}$). The bond lengths of the V−O bonds vary minimally across the series for the solid state monomeric or dimeric species (Table 1). Direct binding of a Lewis acid to an oxo-metal fragment has been shown to result

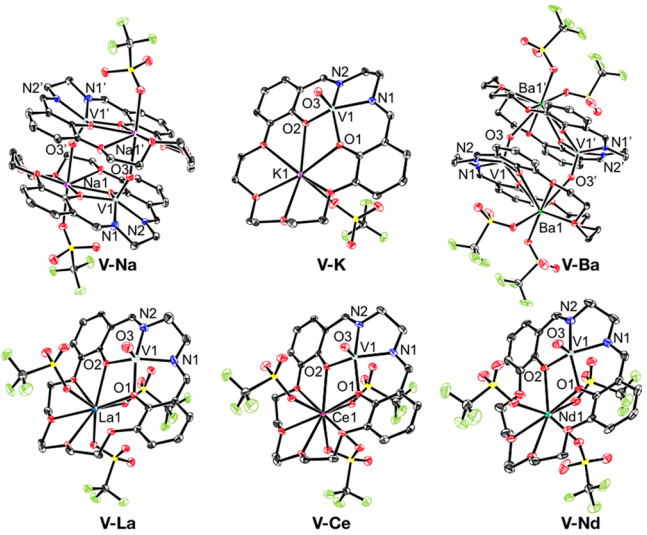


**Figure 1.** Solid-state molecular structures of vanadyl complexes at 50% probability ellipsoids. Hydrogen atoms omitted for clarity. See Table 1 for selected bond metrics.

in significant elongation of the M−O bond.[63−65] For the crown complexes presented here, we observe a slight increase in the V−O bond lengths for V-Na, V-K, V-Ba, and V-La, but the V−O bond lengths of V-Ce and V-Nd are within error of the V−O length for (salen-OMe)V(O). All complexes exhibit distorted square pyramidal geometry with $\tau_5$ values ranging between 0.01 and 0.14. The vanadium atom is displaced toward the apical oxygen atom away from the basal plane (defined by the salen $N_2O_2$ atoms) in all complexes. The V-Nd compound had significant disorder in the crystal structure.

**Cyclic Voltammetry.** Understanding solvent effects when charge is present is critical for ion-pairing and solvent screening as it relates to redox properties and reactivity.[69] Cyclic voltammetry experiments for the series of vanadyl complexes were conducted in solvents of varying polarity as measured by the solvents' dielectric constants ($\varepsilon$). Acetonitrile (MeCN) and *N*,*N*-dimethylformamide (DMF) have similar dielectric constants of 37.5 and 36.7, respectively, and dichloromethane (DCM) has a dielectric constant of 8.93.[70] Cyclic voltammograms of (salen)V(O) (Figure 2, black trace) and (salen-OMe)V(O) (Figure 2, gray trace) exhibit a reversible redox feature at 0.090 and 0.066 V vs $(C_5H_5)_2Fe^{+/0}$, respectively, in 0.1 M tetrabutylammonium hexafluorophosphate ($TBAPF_6$) in MeCN consistent with previously reported values for the vanadium(V/IV) reduction potential.[71]

The electrochemical properties of V-M (M = $Na^+$, $K^+$, $Ba^{2+}$, $Nd^{3+}$, $La^{3+}$) were also measured in MeCN (Figure 2), and


https://doi.org/10.1021/acs.jpca.3c00827
J. Phys. Chem. A 2023, 127, 5324−5334

**Table 1. Summary of Structural Parameters of Vanadyl Complexes**

| complex | V−O bond (Å) | V−M distance (Å) | cation M radius[a] (Å) | $\tau_5$ | displacement of V from basal plane ($N_2O_2$; Å) |
|---|---|---|---|---|---|
| (salen)V(O)[b] | 1.590(1) | | | 0.18 | 0.589 |
| (salen-OMe)V(O)[c] | 1.590(3) | | | 0.13 | 0.589 |
| V-Na | 1.5986(15) | 3.4850(10) | 1.02 | 0.01 | 0.518 |
| V-K | 1.6025(10) | 3.8076(4) | 1.38 | 0.14 | 0.613 |
| V-Ba | 1.6059(11) | 3.7983(3) | 1.35 | 0.12 | 0.610 |
| V-La | 1.600(3) | 3.5980(7) | 1.03 | 0.12 | 0.492 |
| V-Ce | 1.588(2) | 3.6100(6) | 1.01 | 0.10 | 0.485 |
| V-Nd | 1.586(3) | 3.59569(17) | 0.98 | 0.10 | 0.492 |

[a]Values from ref 66. [b]Values from ref 67. [c]Values from ref 68.

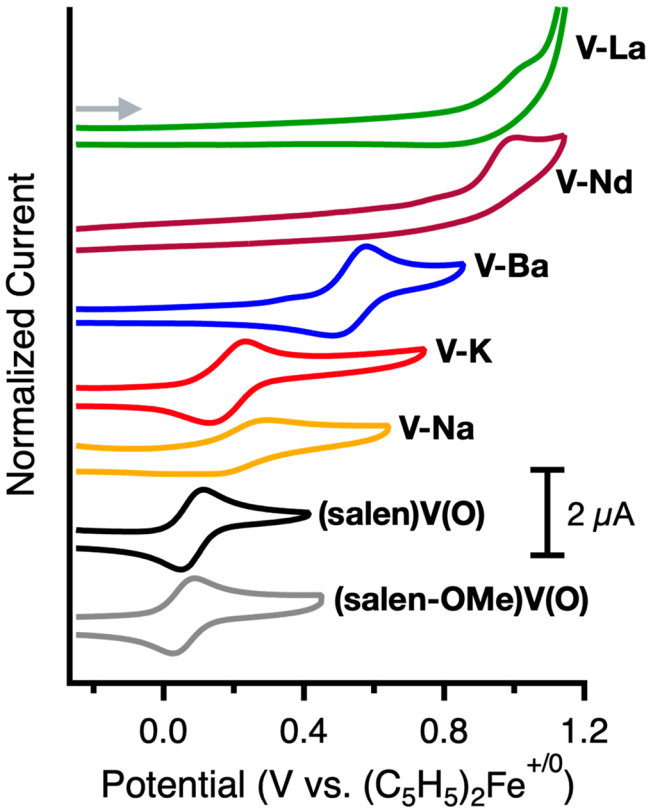


**Figure 2.** Cyclic voltammograms of (salen)V(O), (salen-OMe)V(O), and V-M (M = $Na^+$, $K^+$, $Ba^{2+}$, $Nd^{3+}$, and $La^{3+}$; 0.5 mM) in 0.1 M $TBAPF_6$ in MeCN under $N_2$ showing the vanadium(V/IV) redox couple. Scan rate is 100 mV/s. Decamethylferrocene ($((CH_3)_5C_5)_2Fe$) was used as internal reference and all potentials are reported vs the $(C_5H_5)_2Fe^{+/0}$ redox couple.[53] Arrow indicates scan direction (anodic).

values for the vanadium(V/IV) $E_{1/2}$ are listed in Table 2. The complexes behave as monomers in solution at 23 °C, as indicated by the solution state Evans method magnetic moment measurements, and $^{19}F$ NMR in $CD_3CN$ shows that the triflate anion dissociates in solution (see SI). The vanadium(V/IV) redox event for V-Na, V-K, and V-Ba is reversible and shifts anodically with an increase in the cation charge, consistent with the effect on other heterobimetallic complexes in this ligand framework.[35−39,42−45,72−74] Computational studies were also performed, and the same trend is observed, though the simple model used in the calculations overestimates the increase in $E_{1/2}$ as the cation charge increases (see SI for computational details and Table S3 for values). The vanadium(V/IV) reduction potential for the monocations (V-Na and V-K) shifts 90−130 mV more positive than (salen)V(O) and 114−164 mV more positive than (salen-OMe)V(O). For the dication, V-Ba, the vanadium(V/IV) reduction potential shifts 440 mV positive of (salen)V(O) and 464 mV positive of (salen-OMe)V(O). The cyclic voltammograms of V-La and V-Nd showed an irreversible oxidation event ($E_{pa}$) at 1.10 and 1.09 V versus $(C_5H_5)_2Fe^{+/0}$, respectively, indicating chemical instability of the vanadium(V) oxo for these complexes in MeCN. Attempts to isolate the lanthanum containing a vanadium(V) oxo complex following chemical oxidation of V-La with $NOBF_4$ ($E^{o\prime}([NO]^+/NO)$ = 1.00 V vs $(C_5H_5)_2Fe^{+/0}$)[75] were unsuccessful. Differential pulse voltammetry (DPV) of V-La (see SI, Figure S1) showed an additional oxidation feature directly following the vanadium(IV/V) oxidation ($E_{pa}$ > 1.3 V vs $(C_5H_5)_2Fe^{+/0}$) tentatively assigned as formation of the vanadium(V)-phenoxyl radical, in which the salen ligand is oxidized.[76,77] The closeness of these redox features (~200 mV) may contribute to the observed electrochemical and chemical instability in isolating the oxidized V-La species.

Cyclic voltammograms of V-Na, V-Ba, and V-La were measured in 0.1 M $TBAPF_6$ DCM solutions. All three complexes were sparingly soluble in DCM, which has a relatively low dielectric constant ($\varepsilon$) of 8.93. Shifts of 150 mV (V-Na), 365 mV (V-Ba), and 735 mV (V-La) more positive than (salen)V(O) were observed for the vanadium(V/IV) redox couple, correlating with the increase in cation charge (Table 2, see SI, Figure S2). The vanadium(V/IV) couple for V-K and V-Ba appeared reversible, but V-La showed an irreversible oxidation, similar to its behavior in MeCN.

The electrochemical behavior of the vanadyl complexes measured by cyclic voltammetry in 0.1 M $TBAPF_6$ DMF solutions was markedly different than that observed in either MeCN or DCM. The vanadium(V/IV) redox couple was relatively insensitive to cation bound in the crown, only varying 124 mV across the series compared to the >900 mV and >700 mV shifts observed in MeCN and DCM, respectively (Figure 3). Cyclic voltammetry of related heterobimetallic salen-crown complexes measured in DMF were previously shown to exhibit a positive shift in potential correlated with cation charge.[35,39] Therefore, we further probed the interaction of DMF at vanadium through electrochemical techniques (*vide infra*).

**Cation, Anion, and Solvent Binding at Vanadyl Complexes.** Previous electrochemical studies on vanadyl salen complexes show that solvent polarity and electrolyte interactions can greatly impact the redox behavior[71] and catalytic oxidation reactivity.[62,79−81] Square pyramidal vanadyl salen complexes possess an empty coordination site trans to the oxo group, and upon oxidation, the more electron deficient vanadium(V) typically favors a six-coordinate geometry instead


https://doi.org/10.1021/acs.jpca.3c00827
J. Phys. Chem. A 2023, 127, 5324−5334

**Table 2. Summary of Electrochemical Data for Vanadyl Complexes**

| complex | $E_{1/2}$ V(V/IV) (V), MeCN[a] | $E_{1/2}$ V(V/IV) (V), DCM[a] | $E_{1/2}$ V(V/IV) (V), DMF[a] | p$K_a$ of M($OH_2$) (aq.)[b] | log($K_{DMF}$) |
|---|---|---|---|---|---|
| (salen)V(O) | 0.090 | 0.045 | −0.10 | | 1.75 |
| (salen-OMe)V(O) | 0.066 | | −0.13 | | |
| (salen-crown)V(O) | | | −0.12 | | |
| V-Na | 0.23 | 0.20 | −0.050 | 14.8 | |
| V-K | 0.18 | | −0.036 | 16.3 | 1.90 |
| V-Ba | 0.53 | 0.41 | 0.39, −0.11[c] | 13.4 | 3.67 |
| V-La | 1.10[d] | 0.78[d] | −0.16 | 9.06 | 7.42 |
| V-Ce | | | −0.16 | 9.3 | |
| V-Nd | 1.09[d] | | | 8.4 | |

[a]Reduction potentials referenced to $(C_5H_5)_2Fe^{+/0}$ couple. [b]Values from ref 78. [c]The redox events are quasireversible at all scan rates sampled, so in lieu of reporting $E_{1/2}$, the values reported here correspond to $E_{pa}$ and $E_{pc}$ potentials, for the irreversible oxidation and reduction events, respectively. [d]The redox event is irreversible, so the reported potentials correspond to an $E_{pa}$ for the irreversible oxidation to the vanadium(V) species.

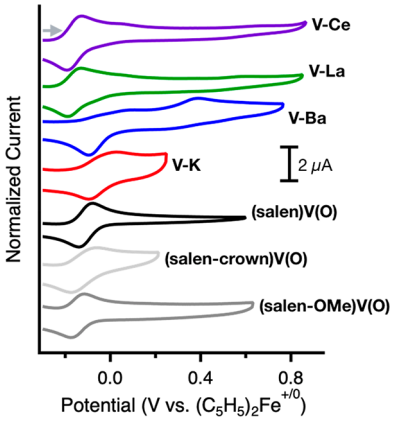


**Figure 3.** Cyclic voltammograms of (salen)V(O), (salen-OMe)V(O), (salen-crown)V(O), and V-M (M = $K^+$, $Ba^{2+}$, $La^{3+}$, $Ce^{3+}$) (0.5 mM) in 0.1 M $TBAPF_6$ in DMF under $N_2$ showing vanadium(V/IV) redox couple. Scan rate is 100 mV/s. Decamethylferrocene ($((CH_3)_5C_5)_2Fe$) was used as internal reference and all potentials are reported vs the $(C_5H_5)_2Fe^{+/0}$ redox couple. Arrow indicates the scan direction (anodic).

of five. This empty coordination site can readily bind coordinating solvents or Lewis bases at the axial position.[82] Previous studies have investigated association of weakly binding anions at this position.[83−85] Additionally, formation of dimeric or oligomeric chains with V−O−V−O linkages have been observed under acidic conditions.[86−89]

We looked to directly probe electrolyte, anion, and solvent interactions at the vanadyl salen-crown complexes in an attempt to better understand their electrochemical behavior in DMF. Cyclic voltammograms of V-K, V-Ba, and V-La measured using the corresponding $M(OTf)_n$ ($M^{n+}$ = $K^+$, $Ba^{2+}$, or $La^{3+}$) as electrolyte (200:1 electrolyte to analyte) in DMF again showed no clear trend in positive potential shift with increased cation charge (SI, Figure S3). Cation binding in the crown ether macrocycle can typically be probed through titration of the $M(OTf)_n$ salt into solution;[90] however, the redox potentials remain consistent even in the presence of a large excess of Lewis acid. Therefore, we conclude that cation dissociation in DMF is not responsible for the lack of anodic shifts.

An electrolyte anion could also bind, complicating the interpretation of the electrochemical measurements. $^{19}F$ NMR of the V-M complexes in DMF-$d_6$ showed that the triflate anion is outer sphere and matches well against a standard of tetrabutylammonium triflate (TBAOTf) (see SI). Cyclic voltammetry of V-La with 0.1 M tetrabutylammonium tetraphenylborate ($TBABPh_4$) electrolyte in DMF showed minimal difference on the vanadium(V/IV) reduction potential ($E_{1/2}$ = −0.16 V vs $(C_5H_5)_2Fe^{+/0}$). $TBABPh_4$ was used because it is a bulkier and relatively less coordinating electrolyte than $TBAPF_6$ or the $M(OTf)_n$ salts. The effect of anion dissociation in DMF was also explored as a reason for the lack of positive redox shift for V-La by cyclic voltammetry. Comparing reduction potentials of $[V\text{-}La][OTf]_3$ and $[V\text{-}La][Cl]_3$ in DMF with 0.1 M $TBABPh_4$ electrolyte exhibited no difference by cyclic voltammetry despite the chloride being a more strongly coordinating anion than triflate (SI, Figure S4). The invariant reduction potentials in the presence of different electrolytes and counter anions indicate another interaction is responsible for the lack of positive shift in DMF.

The differences in the cyclic voltammograms of the vanadium complexes in MeCN versus DMF cannot be explained by dielectric constant of the solvent because the values are similar ($\varepsilon$ = 37.5 and 36.7, respectively), and redox potentials computed with DFT and continuum solvent models are very similar for the two solvents (see SI for computational details). Instead, a better descriptor to consider is the difference in Lewis basicity of the solvents. The Gutmann donor number is a quantitative measure of Lewis basicity.[91−93] The donor numbers for MeCN (14.1 kcal/mol) and DMF (26.6 kcal/mol) correspond with the computed solvent molecule binding energies, which are roughly twice as strong for DMF. The vanadyl complexes offer several possible sites of interaction for a Lewis base, either at the vanadium center or through solvation of the Lewis acid cation. To determine whether DMF coordination plays a role, its binding constant in MeCN for the different complexes was determined. Cyclic voltammograms of the vanadyl complexes, (salen)V(O), V-K, V-Ba, and V-La, were taken at varying concentrations of DMF in MeCN. In all cases, the vanadium(V/IV) reduction potential shifted cathodically with increasing concentrations of DMF (Figure 4). Further, for V-La, the redox couple became reversible at concentrations of 0.1 M DMF and above. This cathodic shift can be explained by DMF binding at the vanadium axial position, thus increasing electron density at the metal center and making it easier to oxidize vanadium(IV) to the vanadium(V) oxidation state. Binding constants for DMF (log($K_{DMF}$)) were calculated using a modified form of the Nernst eq (eq 1), where a plot of $E_{1/2}$ versus log[DMF] gives a linear relationship.[94,95]


https://doi.org/10.1021/acs.jpca.3c00827
J. Phys. Chem. A 2023, 127, 5324−5334

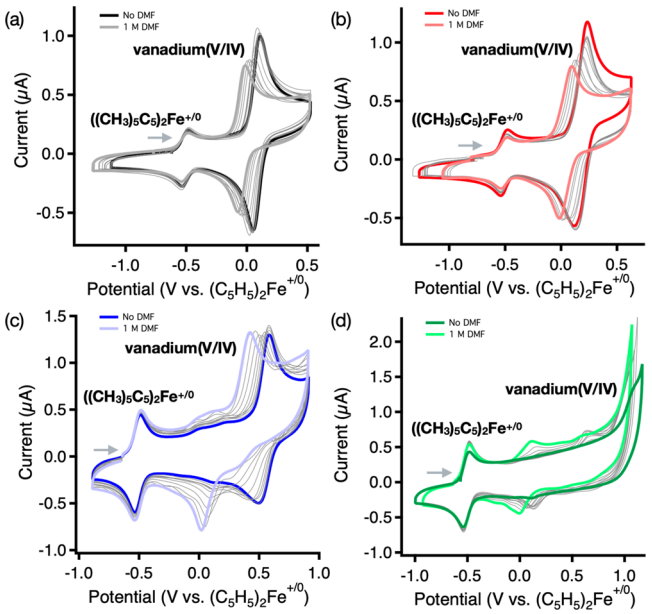


**Figure 4.** Cyclic voltammetry of (a) (salen)V(O), (b) V-K, (c) V-Ba, and (d) V-La with an increasing concentration of DMF. All voltammograms were recorded using MeCN containing 0.1 M $TBAPF_6$ electrolyte and 0.5 mM vanadium analyte. The reversible redox feature at $E_{1/2} = -0.51$ V is $((CH_3)_5C_5)_2Fe$ and was used as an internal standard. Scan rate is 100 mV/s. Arrow indicates the scan direction (anodic).

$$\Delta E_{1/2} = q\frac{0.0592}{n}\log[\mathrm{DMF}] + \frac{0.0592}{n}\log(K_{\mathrm{DMF}}) \quad (1)$$

In eq 1, $q$ is the number of DMF molecules bound and $n$ refers to the number of electrons involved in the redox event. For the one electron oxidation of vanadium(IV) to vanadium(V), the value of $\log(K_{\mathrm{DMF}})$ increases as cation charge increases (Table 2). Further, the slope obtained from these data can be used to determine the number of DMF molecules bound. In the case of (salen)V(O), there should be only one empty coordination site for DMF, and the slope value of 0.05 V/decade is consistent with the binding of one molecule of DMF (see SI, Figure S5). For the V-M complexes, the Lewis acidic metal cation provides an additional binding site. A similar analysis of the slopes for V-K, V-Ba, and V-La suggests that more than one molecule of DMF could be binding. Therefore, binding of multiple DMF molecules at these complexes cannot be ruled out.

Computed binding energies for the two possible binding sites (either V or K/Ba/La) for one DMF molecule suggest that for the V-K complex the two sites bind DMF equally strongly (Figure 5, SI, Table S4), and that for V-Ba and V-La,

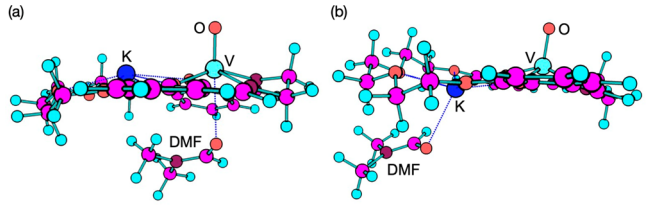


**Figure 5.** Side-on views of computed structures of V-K with (a) a DMF molecule bound to vanadium and (b) a DMF molecule bound to potassium cation.

the Ba/La cations bind DMF more strongly. Furthermore, DMF binding to either site reduces the DFT computed redox potential (e.g., for V-K, DMF binding reduces the reduction potential from 1.05 to 0.85 V (vanadium-bound) or 0.84 V (potassium-bound; SI, Table S5). These calculations confirm that binding of multiple DMF molecules is a probable factor in the observed CV/titration behavior.

The interaction of Lewis acidic metals with the methoxy substituted complex, (salen-OMe)V(O), was also explored. Interactions with salen vanadium oxo complexes with rare earth metals[96] and Group 14 and Group 15 Lewis acids[68] have previously been observed. Two different sites of interaction are possible, through the oxo group or through the methoxy substituents, more akin to the salen−crown complexes. A more electrophilic vanadyl center would disfavor association through the oxo unit. Cyclic voltammograms of (salen-OMe)V(O) were taken at different concentrations of $M(OTf)_n$ salt ($M^{n+}$ = $K^+$, $Ba^{2+}$, $La^{3+}$) with 0.1 M $TBAPF_6$ in MeCN (Figure 6). The

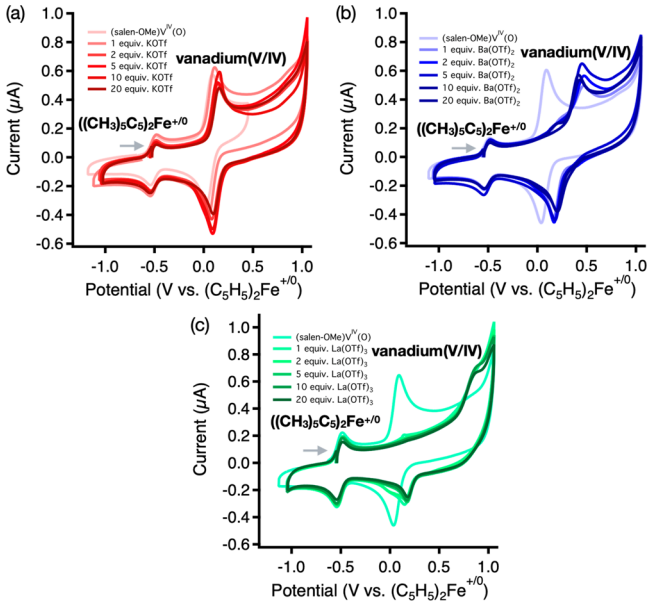


**Figure 6.** Cyclic voltammetry of (salen-OMe)V(O) with titration of (a) KOTf, (b) $Ba(OTf)_2$, or (c) $La(OTf)_3$ salts. Scan rate at 100 mV/s in MeCN and 0.1 M $TBAPF_6$ electrolyte. Redox feature at $E_{1/2} = -0.51$ V is decamethylferrocene ($((CH_3)_5C_5)_2Fe$) used as an internal standard.

vanadium(IV/V) oxidation ($E_{pa}$) for (salen-OMe)V(O) shifted anodically in the presence of the exogenous $M(OTf)_n$ salts, where the maximum $\Delta E_{pa}$ observed was 0.082, 0.37, and 0.80 V for K(OTf), $Ba(OTf)_2$, and $La(OTf)_3$, respectively. However, the $E_{pc}$ (vanadium(V/IV) reduction) of (salen-OMe)V(O) was shifted anodically by a smaller amount, where $\Delta E_{pc}$ was 0.069, 0.16, and 0.14 V for K(OTf), $Ba(OTf)_2$, and $La(OTf)_3$, respectively (Table 3). The asymmetry observed in the magnitude of the shift at the two redox features may be attributed to charge repulsion between the cationic vanadium(V) and the Lewis acidic metal, leading to a weaker association.

**Electronic Absorption and Vibrational Spectroscopy.** The UV−visible spectra of the V-M complexes were explored in both MeCN and DMF (see SI for full spectra). Table 4 lists a summary of UV−visible spectroscopy. There are two major absorption bands observed for all complexes, with an intense


https://doi.org/10.1021/acs.jpca.3c00827
J. Phys. Chem. A 2023, 127, 5324−5334

**Table 3. Summary of Changes in the Anodic and Cathodic Potential upon Titration of (salen-OMe)V(O) with $M(OTf)_n$ ($M^{n+}$ = $K^+$, $Ba^{2+}$, $La^{3+}$) Salts[a]**

| | K(OTf) | | $Ba(OTf)_2$ | | $La(OTf)_3$ | |
|---|---|---|---|---|---|---|
| equiv salt added | $\Delta E_{pa}$ (V) | $\Delta E_{pc}$ (V) | $\Delta E_{pa}$ (V) | $\Delta E_{pc}$ (V) | $\Delta E_{pa}$ (V) | $\Delta E_{pc}$ (V) |
| 0 | 0 | 0 | 0 | 0 | 0 | 0 |
| 1 | 0.020 | 0.014 | 0.37 | 0.12 | 0.79 | 0.11 |
| 2 | 0.025 | 0.030 | 0.37 | 0.13 | 0.79 | 0.12 |
| 5 | 0.045 | 0.051 | 0.37 | 0.14 | 0.80 | 0.14 |
| 10 | 0.058 | 0.058 | 0.33 | 0.16 | 0.79 | 0.14 |
| 20 | 0.082 | 0.069 | 0.32 | 0.16 | 0.79 | 0.14 |

[a]Reduction potentials referenced to $(C_5H_5)_2Fe^{+/0}$ couple. Potential shifts are reported relative to (salen-OMe)V(O) without $M(OTf)_n$ salt.

band at ~360 nm corresponding to a mixed $\pi-\pi^*$/charge transfer (CT) transition and a weaker band at ~580 nm corresponding to vanadium(IV) d−d transitions.[82] A slight red shift was observed in DMF for the $\pi-\pi^*$ band that was more pronounced for complexes containing a cation, and this shift may be due to stabilization by DMF coordination. Spectroelectrochemical UV−vis studies were also used to further investigate the stability of the vanadium complexes following oxidation in both MeCN and DMF. A controlled potential electrolysis ~200 mV positive of the vanadium(V/IV) reduction potential was applied in 0.2 M $TBAPF_6$ solutions and UV−vis spectra were collected at 1 s intervals during electrolysis. In MeCN, (salen)V(O), V-K, and V-Ba all showed the growth of a broad absorbance peak between 600 and 800 nm corresponding to a charge transfer band associated with formation of the vanadium(V) species (Figure S21). The UV−vis spectrum of V-La in MeCN under electrolysis only showed decomposition, further supporting the instability and inaccessibility of the vanadium(V) for the lanthanum-containing complex. In DMF, however, the growth of the charge transfer band was observed for V-K, V-Ba, and V-La, indicating that bound DMF may be stabilizing the vanadium-(V) species, supporting the reversibility observed for the vanadium(V/IV) redox couple in DMF solutions (see SI, Figure S22).

Vibrational resonances shift in response to an electrostatic field due to the Stark effect.[98] The solid-state infrared (IR) spectra for the vanadyl salen-crown complexes have V≡O stretching frequencies that increase by 32 $cm^{-1}$ and the imine C═N bond frequencies by 42 $cm^{-1}$ over the series of complexes. Plotting the vibrational data against the $E_{1/2}$ data collected in different solvents shows that a positive linear correlation is present in MeCN and DCM consistent with a vibrational Stark effect, however in DMF no positive correlation is observed (Figure 7). The lack of positive

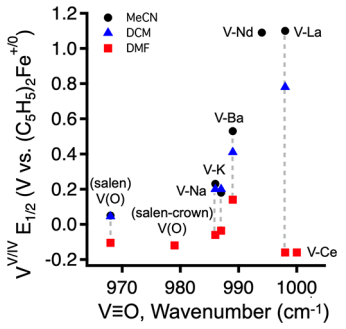


**Figure 7.** Plot showing vibrational Stark effect for vanadyl salen-crown complexes where there is a positive correlation between the V≡O stretching frequency and vanadium(V/IV) reduction potential in MeCN and DCM. However, this positive correlation is quenched in DMF.

correlation in DMF again may be a consequence of DMF binding to either the vanadium center or Lewis acidic metal cation. Similar increases in the V≡O and C═N bond frequencies for the V-M complexes are observed in the solution state IRs, confirming that the positive correlations hold for the solvated complexes in MeCN and DCM, but not for DMF (see SI, Table S1 and Figure S24).

## IV. CONCLUSIONS

These studies indicate that solvation effects and Lewis basic behavior by DMF can effectively mitigate Lewis acidic metal charge effects on reduction potentials. Cyclic voltammetry and UV−visible spectroscopy confirmed that DMF can act as a ligand. The binding constant of DMF increases as the cation charge increases, consistent with a stronger Lewis acid/base interaction and increasing electron density at the metal center as measured by the reduction potentials. In MeCN, incorporation of charge leads to a positive shift in reduction potential for the vanadium(V/IV) couple by >900 mV. However, in DMF the reduction potential only shifts by 124 mV across the series of complexes investigated.

We observe that the interplay of electrostatics and Lewis acidic interactions are highly depended on solvent and electrolyte in solution. For the vanadyl complexes, the Lewis acid/base interaction dominates in DMF, due to its donor ability (as expressed by the Gutmann donor number). In

**Table 4. Summary of Electronic Absorbance and Vibrational Spectroscopy**

| complex | MeCN $\lambda$/nm ($\varepsilon/M^{-1}$ $cm^{-1}$) | DMF $\lambda$/nm ($\varepsilon/M^{-1}$ $cm^{-1}$) | $\upsilon$(V≡O) ($cm^{-1}$) | $\upsilon$(C═N) ($cm^{-1}$) |
|---|---|---|---|---|
| (salen)V(O) | 365 (9600), 590 (210) | 363 (6075), 587 (123)[a] | 968 | 1531 |
| (salen-OMe)V(O) | 360 (5600), 600 (200) | | 976 | 1522 |
| (salen-crown)V(O) | | 376 (3400), 598 (110) | 979 | 1525 |
| V-Na | 374 (2500), 592 (60) | 378 (2990), 594 (70) | 986 | 1554 |
| V-K | 374 (23,500), 584 (160) | 376 (3900), 572 (90) | 987 | 1553 |
| V-Ba | 366 (4400), 588 (70) | 382 (5600), 578 (110) | 989 | 1557 |
| V-La | 354 (4000), 610 (60) | 378 (6300), 602 (170) | 998 | 1563 |
| V-Ce | 354 (3900), 604 (170) | 380 (9300), 592 (280) | 1000 | 1564 |
| V-Nd | 346 (4700), 596 (180) | 386 (3100), 598 (80) | 994 | 1530 |

[a]Values from ref 97.



https://doi.org/10.1021/acs.jpca.3c00827
J. Phys. Chem. A 2023, 127, 5324−5334

acetonitrile and DCM, the positive redox shifts observed in the cyclic voltammetry data, as well as the vibrational stretching frequencies are most consistent with an electrostatic effect, although we cannot completely rule out any Lewis acidic effects in these solvents.

We have also demonstrated that addition of exogenous triflate salt to (salen-OMe)V(O) in MeCN produces a positive shift in the vanadium(V/IV) reduction potential, but charge repulsion upon oxidation to vanadium(V) results in cation dissociation and a loss of reversibility by cyclic voltammetry. The crown is essential for maintaining Lewis acid metal coordination and mitigating charge repulsion. The impact of these studies shows that electrostatic and Lewis acidic effects are dependent on solvent choice and coordination environment, informing future work on considering these interactions to enhance cationic interactions and improve catalyst design.

## ■ ASSOCIATED CONTENT

### Supporting Information

The Supporting Information is available free of charge at https://pubs.acs.org/doi/10.1021/acs.jpca.3c00827.

Experimental crystallographic data for V-Na (CIF)

Experimental crystallographic data for V-K (CIF)

Experimental crystallographic data for V-Ba (CIF)

Experimental crystallographic data for V-La (CIF)

Experimental crystallographic data for V-Nd (CIF)

Experimental crystallographic data for V-Ce (CIF)

Cartesian coordinates (*xyz*) for all computationally optimized structures used for computed reduction potentials and solvent binding models (ZIP)

Synthetic details for salen-crown-M ligands and vanadium complexes (V-M); electrochemical analysis; spectroscopic data for V-M complexes (UV−vis, IR, EPR, and NMR); summary of computational results, computed reduction potentials, and binding energies; plots of crystallographic data (PDF)

## ■ AUTHOR INFORMATION


### Corresponding Authors

**Nadia G. Léonard** − *Department of Chemistry, University of California, Irvine, Irvine, California 92697, United States;* orcid.org/0000-0002-0949-5471; Email: leonarn1@uci.edu

**Anastassia N. Alexandrova** − *Department of Chemistry and Biochemistry, University of California, Los Angeles, Los Angeles, California 90095, United States;* orcid.org/0000-0002-3003-1911; Email: ana@chem.ucla.edu

### Authors

**Hien M. Nguyen** − *Department of Chemistry, University of California, Irvine, Irvine, California 92697, United States;* orcid.org/0000-0001-9634-3427

**Harry W. T. Morgan** − *Department of Chemistry and Biochemistry, University of California, Los Angeles, Los Angeles, California 90095, United States;* orcid.org/0000-0001-9647-8807

**Teera Chantarojsiri** − *Department of Chemistry and Center of Excellence for Innovation in Chemistry, Faculty of Science, Mahidol University, Bangkok 10400, Thailand;* orcid.org/0000-0002-4951-9503

**Tyler A. Kerr** − *Department of Chemistry, University of California, Irvine, Irvine, California 92697, United States;* orcid.org/0000-0002-0369-4883

**Jenny Y. Yang** − *Department of Chemistry, University of California, Irvine, Irvine, California 92697, United States;* orcid.org/0000-0002-9680-8260

Complete contact information is available at: https://pubs.acs.org/10.1021/acs.jpca.3c00827


### Notes

The authors declare no competing financial interest.

## ■ ACKNOWLEDGMENTS

T.C. was supported by NSF Award #15554744 and N.G.L. by NIH 3R01GM134047-02S1. N.G.L. would also like to acknowledge support from the UC Presidential Postdoctoral Fellowship Program. J.Y.Y. also acknowledges support as a Sloan Foundation Fellow, a Canadian Institute for Advanced Research (CIFAR) Azrieli Global Scholar in the Bio-Inspired Solar Energy Program, and a Camille Dreyfus Teacher Scholar. A.N.A. acknowledges support from NSF CHE Grant 22-3366. The authors acknowledge computational resources from the National Energy Research Scientific Computing Center (NERSC), a U.S. Department of Energy Office of Science User Facility located at Lawrence Berkeley National Laboratory, and DOE-BES Grant DE-SC0019152.

## ■ REFERENCES


(1) Sutradhar, M.; Martins, L. M. D. R. S.; Guedes da Silva, M. F. C.; Pombeiro, A. J. L. Vanadium Complexes: Recent Progress in Oxidation Catalysis. *Coord. Chem. Rev.* **2015**, *301*−*302*, 200−239.

(2) da Silva, J. A. L.; da Silva, J. J. R. F.; Pombeiro, A. J. L. Oxovanadium Complexes in Catalytic Oxidations. *Coord. Chem. Rev.* **2011**, *255* (19), 2232−2248.

(3) Zhang, Y.; Holm, R. H. Vanadium-Mediated Oxygen Atom Transfer Reactions. *Inorg. Chem.* **1990**, *29* (5), 911−917.

(4) Belokon, Y. N.; Maleev, V. I.; North, M.; Usanov, D. L. VO(Salen)(X) Catalysed Asymmetric Cyanohydrin Synthesis: An Unexpected Influence of the Nature of Anion X on the Catalytic Activity. *Chem. Commun.* **2006**, *44*, 4614−4616.

(5) Belokon, Y. N.; Clegg, W.; Harrington, R. W.; Maleev, V. I.; North, M.; Pujol, M. O.; Usanov, D. L.; Young, C. Mechanism-Guided Development of VO(Salen)X Complexes as Catalysts for the Asymmetric Synthesis of Cyanohydrin Trimethylsilyl Ethers. *Chem.—Eur. J.* **2009**, *15* (9), 2148−2165.

(6) Xi, W.; Liu, Y.; Xia, Q.; Li, Z.; Cui, Y. Direct and Post-Synthesis Incorporation of Chiral Metallosalen Catalysts into Metal−Organic Frameworks for Asymmetric Organic Transformations. *Chem.—Eur. J.* **2015**, *21* (36), 12581−12585.

(7) Gandeepan, P.; Müller, T.; Zell, D.; Cera, G.; Warratz, S.; Ackermann, L. 3d Transition Metals for C−H Activation. *Chem. Rev.* **2019**, *119* (4), 2192−2452.

(8) Zhang, G.; Wu, J.; Zheng, S.; Neary, M. C.; Mao, J.; Flores, M.; Trovitch, R. J.; Dub, P. A. Redox-Noninnocent Ligand-Supported Vanadium Catalysts for the Chemoselective Reduction of C═X (X = O, N) Functionalities. *J. Am. Chem. Soc.* **2019**, *141* (38), 15230−15239.

(9) Białek, M.; Leksza, A.; Piechota, A.; Kurzak, K.; Koprek, K. Oxovanadium(IV) Complexes with [ONNO]-Chelating Ligands as Catalysts for Ethylene Homo- and Copolymerization. *J. Polym. Res.* **2014**, *21* (4), 389.

(10) Waidmann, C. R.; DiPasquale, A. G.; Mayer, J. M. Synthesis and Reactivity of Oxo-Peroxo-Vanadium(V) Bipyridine Compounds. *Inorg. Chem.* **2010**, *49* (5), 2383−2391.

(11) Radosevich, A. T.; Musich, C.; Toste, F. D. Vanadium-Catalyzed Asymmetric Oxidation of α-Hydroxy Esters Using

Molecular Oxygen as Stoichiometric Oxidant. *J. Am. Chem. Soc.* **2005**, *127* (4), 1090−1091.
(12) Shi, M.; Xu, B. VO(Acac)2-Catalyzed Oxidative Coupling Reactions of Phosphonium Salts. *J. Org. Chem.* **2002**, *67* (1), 294−297.
(13) Ishikawa, T.; Ogawa, A.; Hirao, T. Oxovanadium(V)-Induced Oxidative Coupling of Organolithium and -Magnesium Compounds. *Organometallics* **1998**, *17* (26), 5713−5716.
(14) Hirao, T. Vanadium in Modern Organic Synthesis. *Chem. Rev.* **1997**, *97* (8), 2707−2724.
(15) Galloni, P.; Conte, V.; Floris, B. A Journey into the Electrochemistry of Vanadium Compounds. *Coord. Chem. Rev.* **2015**, *301−302*, 240−299.
(16) Tsuchida, E.; Yamamoto, K.; Oyaizu, K.; Iwasaki, N.; Anson, F. C. Electrochemical Investigations of the Complexes Resulting from the Acid-Promoted Deoxygenation and Dimerization of (N,N'-Ethylenebis(Salicylideneaminato))Oxovanadium(IV). *Inorg. Chem.* **1994**, *33* (6), 1056−1063.
(17) Del Carpio, E.; Hernández, L.; Ciangherotti, C.; Villalobos Coa, V.; Jiménez, L.; Lubes, V.; Lubes, G. Vanadium: History, Chemistry, Interactions with α-Amino Acids and Potential Therapeutic Applications. *Coord. Chem. Rev.* **2018**, *372*, 117−140.
(18) Pessoa, J. C.; Etcheverry, S.; Gambino, D. Vanadium Compounds in Medicine. *Coord. Chem. Rev.* **2015**, *301−302*, 24−48.
(19) Mjos, K. D.; Orvig, C. Metallodrugs in Medicinal Inorganic Chemistry. *Chem. Rev.* **2014**, *114* (8), 4540−4563.
(20) Muhammad, N.; Ali, S.; Shahzadi, S.; Khan, A. N. Oxovanadium(IV) Complexes of Non-Steroidal Anti-Inflammatory Drugs: Synthesis, Spectroscopy, and Antimicrobial Activity. *Russ J. Coord Chem.* **2008**, *34* (6), 448−453.
(21) Thompson, K. H.; Orvig, C. Coordination Chemistry of Vanadium in Metallopharmaceutical Candidate Compounds. *Coord. Chem. Rev.* **2001**, *219−221*, 1033−1053.
(22) Pessoa, J. C.; Correia, I. Salan vs. Salen Metal Complexes in Catalysis and Medicinal Applications: Virtues and Pitfalls. *Coord. Chem. Rev.* **2019**, *388*, 227−247.
(23) Matsuoka, N.; Tsuchimoto, M.; Yoshioka, N. Theoretical Study of Magnetic Properties of Oxovanadium(IV) Complex Self-Assemblies with Tetradentate Schiff Base Ligands. *J. Phys. Chem. B* **2011**, *115* (26), 8465−8473.
(24) Matsuoka, N.; Kawamura, H.; Yoshioka, N. Magnetic Property and Crystal Structure of Bis [N-(4-Chlorophenyl) Salicylideneaminato] Oxovanadium (IV). *Chem. Phys. Lett.* **2010**, *488* (1), 32−37.
(25) Takano, K.; Sunatsuki, Y.; Kojima, M.; Kinoshita, I.; Shibahara, T. Synthesis and Characterization of 8-Quinolinolato Vanadium(IV) Complexes. *Inorg. Chim. Acta* **2009**, *362* (9), 3201−3207.
(26) Papoutsakis, D.; Ichimura, A. S.; Young, V. G., Jr.; Jackson, J. E.; Nocera, D. G. Structural and Magnetic Properties of Vanadyl Dichloride Solvates: From Molecular Units to Extended Hydrogen-Bonded Solids. *Dalton Trans.* **2004**, *2*, 224−228.
(27) Ishida, T.; Mitsubori, S.; Nogami, T.; Takeda, N.; Ishikawa, M.; Iwamura, H. Ferromagnetic Exchange Coupling of Vanadium(IV) Dπ Spins across Pyrimidine Rings: Dinuclear Complexes of Oxovanadium(IV) Bis(1,1,1,5,5,5-Hexafluoropentane-2,4-Dionate) Bridged by Pyrimidine Derivatives. *Inorg. Chem.* **2001**, *40* (27), 7059−7064.
(28) Castro, S. L.; Cass, M. E.; Hollander, F. J.; Bartley, S. L. Oxo-Vanadium(IV) Dimer of 3-Hydroxy-3-Methylglutarate: X-Ray Crystal Structure, Solid State Magnetism, and Solution Spectroscopy. *Inorg. Chem.* **1995**, *34* (2), 466−472.
(29) Kotrle, K.; Nemec, I.; Moncol, J.; Čižmár, E.; Herchel, R. 3d−4f Magnetic Exchange Interactions and Anisotropy in a Series of Heterobimetallic Vanadium(IV)−Lanthanide(III) Schiff Base Complexes. *Dalton Trans.* **2021**, *50* (39), 13883−13893.
(30) Liu, Z.; Anson, F. C. Electrochemical Properties of Vanadium-(III,IV,V)−Salen Complexes in Acetonitrile. Four-Electron Reduction of O2 by V(III)−Salen. *Inorg. Chem.* **2000**, *39* (2), 274−280.
(31) Chang, C. J.; Labinger, J. A.; Gray, H. B. Aerobic Epoxidation of Olefins Catalyzed by Electronegative Vanadyl Salen Complexes. *Inorg. Chem.* **1997**, *36* (25), 5927−5930.
(32) Tsui, E. Y.; Agapie, T. Reduction Potentials of Heterometallic Manganese−Oxido Cubane Complexes Modulated by Redox-Inactive Metals. *Proc. Natl. Acad. Sci. U. S. A.* **2013**, *110* (25), 10084−10088.
(33) Park, Y. J.; Cook, S. A.; Sickerman, N. S.; Sano, Y.; Ziller, J. W.; Borovik, A. S. Heterobimetallic Complexes with MIII-(μ-OH)-MII Cores (MIII = Fe, Mn, Ga; MII = Ca, Sr, and Ba): Structural, Kinetic, and Redox Properties. *Chem. Sci.* **2013**, *4* (2), 717−726.
(34) Delgado, M.; Ziegler, J. M.; Seda, T.; Zakharov, L. N.; Gilbertson, J. D. Pyridinediimine Iron Complexes with Pendant Redox-Inactive Metals Located in the Secondary Coordination Sphere. *Inorg. Chem.* **2016**, *55* (2), 555−557.
(35) Reath, A. H.; Ziller, J. W.; Tsay, C.; Ryan, A. J.; Yang, J. Y. Redox Potential and Electronic Structure Effects of Proximal Nonredox Active Cations in Cobalt Schiff Base Complexes. *Inorg. Chem.* **2017**, *56* (6), 3713−3718.
(36) Kumar, A.; Lionetti, D.; Day, V. W.; Blakemore, J. D. Trivalent Lewis Acidic Cations Govern the Electronic Properties and Stability of Heterobimetallic Complexes of Nickel. *Chemistry − A European Journal* **2018**, *24* (1), 141−149.
(37) Chantarojsiri, T.; Ziller, J. W.; Yang, J. Y. Incorporation of Redox-Inactive Cations Promotes Iron Catalyzed Aerobic C−H Oxidation at Mild Potentials. *Chem. Sci.* **2018**, *9* (9), 2567−2574.
(38) Chantarojsiri, T.; Reath, A. H.; Yang, J. Y. Cationic Charges Leading to an Inverse Free-Energy Relationship for N−N Bond Formation by MnVI Nitrides. *Angew. Chem., Int. Ed.* **2018**, *57* (43), 14037−14042.
(39) Kang, K.; Fuller, J.; Reath, A. H.; Ziller, J. W.; Alexandrova, A. N.; Yang, J. Y. Installation of Internal Electric Fields by Non-Redox Active Cations in Transition Metal Complexes. *Chem. Sci.* **2019**, *10* (43), 10135−10142.
(40) Park, D.; Jette, C. I.; Kim, J.; Jung, W.-O.; Lee, Y.; Park, J.; Kang, S.; Han, M. S.; Stoltz, B. M.; Hong, S. Enantioselective Alkynylation of Trifluoromethyl Ketones Catalyzed by Cation-Binding Salen Nickel Complexes. *Angew. Chem., Int. Ed.* **2020**, *59* (2), 775−779.
(41) Deacy, A. C.; Moreby, E.; Phanopoulos, A.; Williams, C. K. Co(III)/Alkali-Metal(I) Heterodinuclear Catalysts for the Ring-Opening Copolymerization of CO2 and Propylene Oxide. *J. Am. Chem. Soc.* **2020**, *142* (45), 19150−19160.
(42) Kumar, A.; Lionetti, D.; Day, V. W.; Blakemore, J. D. Redox-Inactive Metal Cations Modulate the Reduction Potential of the Uranyl Ion in Macrocyclic Complexes. *J. Am. Chem. Soc.* **2020**, *142* (6), 3032−3041.
(43) Kelsey, S. R.; Kumar, A.; Oliver, A. G.; Day, V. W.; Blakemore, J. D. Promotion and Tuning of the Electrochemical Reduction of Hetero- and Homobimetallic Zinc Complexes**. *ChemElectroChem.* **2021**, *8* (15), 2792−2802.
(44) Léonard, N. G.; Chantarojsiri, T.; Ziller, J. W.; Yang, J. Y. Cationic Effects on the Net Hydrogen Atom Bond Dissociation Free Energy of High-Valent Manganese Imido Complexes. *J. Am. Chem. Soc.* **2022**, *144* (4), 1503−1508.
(45) Golwankar, R. R.; Kumar, A.; Day, V. W.; Blakemore, J. D. Revealing the Influence of Diverse Secondary Metal Cations on Redox-Active Palladium Complexes. *Chem.—Eur. J.* **2022**, *28* (38), e202200344.
(46) Léonard, N. G.; Dhaoui, R.; Chantarojsiri, T.; Yang, J. Y. Electric Fields in Catalysis: From Enzymes to Molecular Catalysts. *ACS Catal.* **2021**, *11*, 10923−10932.
(47) Weberg, A. B.; Murphy, R. P.; Tomson, N. C. Oriented Internal Electrostatic Fields: An Emerging Design Element in Coordination Chemistry and Catalysis. *Chem. Sci.* **2022**, *13* (19), 5432−5446.
(48) Hoffmann, N. M.; Wang, X.; Berkelbach, T. C. Linear Free Energy Relationships in Electrostatic Catalysis. *ACS Catal.* **2022**, *12* (14), 8237−8241.
(49) Brianese, N.; Casellato, U.; Tamburini, S.; Tomasin, P.; Vigato, P. A. Asymmetric Compartmental Macrocyclic Ligands and Related


https://doi.org/10.1021/acs.jpca.3c00827
J. Phys. Chem. A 2023, 127, 5324−5334

Mononuclear and Hetero-Dinuclear Complexes with d- and/or f-Metal Ions. *Inorg. Chim. Acta* **1999**, *293* (2), 178−194.
(50) Reath, A. H. Electrostatic Interactions in Heterobimetallic Complexes and Their Effect on Reduction Potentials, Electronic Structure, and Reactivity, UC Irvine, 2019. https://escholarship.org/uc/item/6h72z6hd#author (accessed 2021−07−02).
(51) Stoll, S.; Schweiger, A. EasySpin, a Comprehensive Software Package for Spectral Simulation and Analysis in EPR. *J. Magn. Reson.* **2006**, *178* (1), 42−55.
(52) Molton, F. Simultispin: A Versatile Graphical User Interface for the Simulation of Solid-State Continuous Wave EPR Spectra. *Magn. Reson. Chem.* **2020**, *58* (8), 718−726.
(53) Aranzaes, J. R.; Daniel, M.-C.; Astruc, D. Metallocenes as References for the Determination of Redox Potentials by Cyclic Voltammetry Permethylated Iron and Cobalt Sandwich Complexes, Inhibition by Polyamine Dendrimers, and the Role of Hydroxy-Containing Ferrocenes. *Can. J. Chem.* **2006**, *84* (2), 288−299.
(54) Hay, B. P.; Firman, T. K.; Moyer, B. A. Structural Design Criteria for Anion Hosts: Strategies for Achieving Anion Shape Recognition through the Complementary Placement of Urea Donor Groups. *J. Am. Chem. Soc.* **2005**, *127* (6), 1810−1819.
(55) Krause, L.; Herbst-Irmer, R.; Sheldrick, G. M.; Stalke, D. Comparison of Silver and Molybdenum Microfocus X-Ray Sources for Single-Crystal Structure Determination. *J. Appl. Crystallogr.* **2015**, *48* (1), 3−10.
(56) Sheldrick, G. M. SHELXT − Integrated Space-Group and Crystal-Structure Determination. *Acta Cryst. A* **2015**, *71* (1), 3−8.
(57) Sheldrick, G. M. Crystal Structure Refinement with SHELXL. *Acta Cryst. C* **2015**, *71* (1), 3−8.
(58) Hübschle, C. B.; Sheldrick, G. M.; Dittrich, B. ShelXle: A Qt Graphical User Interface for SHELXL. *J. Appl. Crystallogr.* **2011**, *44* (6), 1281−1284.
(59) Neese, F. The ORCA Program System. *WIREs Computational Molecular Science* **2012**, *2* (1), 73−78.
(60) Lin, Y.-S.; Li, G.-D.; Mao, S.-P.; Chai, J.-D. Long-Range Corrected Hybrid Density Functionals with Improved Dispersion Corrections. *J. Chem. Theory Comput.* **2013**, *9* (1), 263−272.
(61) Weigend, F.; Ahlrichs, R. Balanced Basis Sets of Split Valence, Triple Zeta Valence and Quadruple Zeta Valence Quality for H to Rn: Design and Assessment of Accuracy. *Phys. Chem. Chem. Phys.* **2005**, *7* (18), 3297−3305.
(62) Coletti, A.; Galloni, P.; Sartorel, A.; Conte, V.; Floris, B. Salophen and Salen Oxo Vanadium Complexes as Catalysts of Sulfides Oxidation with H2O2: Mechanistic Insights. *Catal. Today* **2012**, *192* (1), 44−55.
(63) Franceschi, F.; Solari, E.; Floriani, C.; Rosi, M.; Chiesi-Villa, A.; Rizzoli, C. Molecular Batteries Based on Carbon−Carbon Bond Formation and Cleavage in Titanium and Vanadium Schiff Base Complexes. *Chem.—Eur. J.* **1999**, *5* (2), 708−721.
(64) Fukuzumi, S.; Morimoto, Y.; Kotani, H.; Naumov, P.; Lee, Y.-M.; Nam, W. Crystal Structure of a Metal Ion-Bound Oxoiron(IV) Complex and Implications for Biological Electron Transfer. *Nat. Chem.* **2010**, *2* (9), 756−759.
(65) Draksharapu, A.; Rasheed, W.; Klein, J. E. M. N.; Que, L., Jr. Facile and Reversible Formation of Iron(III)−Oxo−Cerium(IV) Adducts from Nonheme Oxoiron(IV) Complexes and Cerium(III). *Angew. Chem., Int. Ed.* **2017**, *56* (31), 9091−9095.
(66) Shannon, R. D. Revised Effective Ionic Radii and Systematic Studies of Interatomic Distances in Halides and Chalcogenides. *Acta Crystallogr., Sect. A* **1976**, *32* (5), 751−767.
(67) Riley, P. E.; Pecoraro, V. L.; Carrano, C. J.; Bonadies, J.; Raymond, K. N. X-Ray Crystallographic Characterization of a Stepwise, Metal-Assisted Oxidative Decarboxylation: Vanadium Complexes of Ethylenebis[(o-Hydroxyphenyl)Glycine] and Derivatives. *Inorg. Chem.* **1986**, *25* (2), 154−160.
(68) Cashin, B.; Cunningham, D.; Daly, P.; McArdle, P.; Munroe, M.; Chonchubhair, N. N. Donor Properties of the Vanadyl Ion: Reactions of Vanadyl Salicylaldimine $\beta$-Ketimine and Acetylacetonato Complexes with Groups 14 and 15 Lewis Acids. *Inorg. Chem.* **2002**, *41* (4), 773−782.
(69) Stelson, A. C.; Hong, C. M.; Groenenboom, M. C.; Little, C. A. E.; Booth, J. C.; Orloff, N. D.; Bergman, R. G.; Raymond, K. N.; Schwarz, K. A.; Toste, F. D.; et al. Measuring Ion-Pairing and Hydration in Variable Charge Supramolecular Cages with Microwave Microfluidics. *Commun. Chem.* **2019**, *2* (1), 1−10.
(70) Buckley, F.; Maryott, A. A. *Standards, U. S. N. B. of Tables of Dielectric Dispersion Data for Pure Liquids and Dilute Solutions*; U.S. Department of Comerce, National Bureau of Standards, 1958.
(71) Galloni, P.; Coletti, A.; Floris, B.; Conte, V. Electrochemical Properties of VO Salen Complexes. *Inorg. Chim. Acta* **2014**, *420*, 144−148.
(72) Sarkar, R. S.; Biswas, A.; Ray, P. P.; Gomila, R. M.; Drew, M. G. B.; Banerjee, S.; Frontera, A.; Chattopadhyay, S. An Insight into the Non-Covalent Interactions in the Solid State Structures of Dinuclear Cobalt(II) Complexes with N,O-Donor Ligands: Application of the Complexes in the Fabrication of Schottky Devices. *CrystEngComm* **2023**, *25*, 1006.
(73) Bhunia, P.; Gomila, R. M.; Frontera, A.; Ghosh, A. Combine Effect of Lewis Acidity and Electric Field of Proximal Redox Innocent Metal Ions on Redox Potential of Vanadyl Schiff Base Complexes: Experimental and Theoretical Study. *Dalton Trans.* **2023**, *52*, 3097.
(74) Das, L. K.; Bhunia, P.; Gomila, R. M.; Frontera, A.; Ghosh, A. Importance of the Non-Covalent Interactions on the Coordination Geometry of Ni(II) in Ni(II)-M(II) Complexes (M = Zn and Hg) with a Salen Type N2O2 Schiff Base Ligand and Thiocyanate as Coligand. *CrystEngComm* **2023**, *25*, 1393.
(75) Connelly, N. G.; Geiger, W. E. Chemical Redox Agents for Organometallic Chemistry. *Chem. Rev.* **1996**, *96* (2), 877−910.
(76) Kurahashi, T.; Fujii, H. One-Electron Oxidation of Electronically Diverse Manganese(III) and Nickel(II) Salen Complexes: Transition from Localized to Delocalized Mixed-Valence Ligand Radicals. *J. Am. Chem. Soc.* **2011**, *133* (21), 8307−8316.
(77) Clarke, R. M.; Herasymchuk, K.; Storr, T. Electronic Structure Elucidation in Oxidized Metal−Salen Complexes. *Coord. Chem. Rev.* **2017**, *352*, 67−82.
(78) Perrin, D. D. *Ionisation Constants of Inorganic Acids and Bases in Aqueous Solution*; Elsevier, 2016.
(79) Menati, S.; Rudbari, H. A.; Khorshidifard, M.; Jalilian, F. A New Oxovanadium(IV) Complex Containing an O,N-Bidentate Schiff Base Ligand: Synthesis at Ambient Temperature, Characterization, Crystal Structure and Catalytic Performance in Selective Oxidation of Sulfides to Sulfones Using H2O2 under Solvent-Free Conditions. *J. Mol. Struct.* **2016**, *1103*, 94−102.
(80) Boghaei, D. M.; Mohebi, S. Synthesis, Characterization and Study of Vanadyl Tetradentate Schiff Base Complexes as Catalyst in Aerobic Selective Oxidation of Olefins. *J. Mol. Catal. A: Chemical* **2002**, *179* (1), 41−51.
(81) Gupta, K. C.; Sutar, A. K. Catalytic Activities of Schiff Base Transition Metal Complexes. *Coord. Chem. Rev.* **2008**, *252* (12), 1420−1450.
(82) Kanso, H.; Clarke, R. M.; Kochem, A.; Arora, H.; Philouze, C.; Jarjayes, O.; Storr, T.; Thomas, F. Effect of Distortions on the Geometric and Electronic Structures of One-Electron Oxidized Vanadium(IV), Copper(II), and Cobalt(II)/(III) Salen Complexes. *Inorg. Chem.* **2020**, *59* (7), 5133−5148.
(83) Oyaizu, K.; Dewi, E. L.; Tsuchida, E. Coordination of BF4- to Oxovanadium(V) Complexes, Evidenced by the Redox Potential of Oxovanadium(IV/V) Couples in CH2Cl2. *Inorg. Chem.* **2003**, *42* (4), 1070−1075.
(84) Fairhurst, S. A.; Hughes, D. L.; Leigh, G. J.; Sanders, J. R.; Weisner, J. Novel Binuclear Vanadium(V)−Schiff Base Cations Containing Single Fluorine Bridges and the Structure of Difluorodioxovanadate(1−). *J. Chem. Soc., Dalton Trans.* **1994**, *18*, 2591−2598.
(85) Chatterjee, P. B.; Abtab, S. M. T.; Bhattacharya, K.; Endo, A.; Shotton, E. J.; Teat, S. J.; Chaudhury, M. Hetero-Bimetallic Complexes Involving Vanadium(V) and Rhenium(VII) Centers,

Connected by Unsupported μ-Oxido Bridge: Synthesis, Characterization, and Redox Study. *Inorg. Chem.* **2008**, *47* (19), 8830−8838.
(86) Tsuchida, E.; Oyaizu, K. Oxovanadium(III−V) Mononuclear Complexes and Their Linear Assemblies Bearing Tetradentate Schiff Base Ligands: Structure and Reactivity as Multielectron Redox Catalysts. *Coord. Chem. Rev.* **2003**, *237* (1), 213−228.
(87) Yamamoto, K.; Oyaizu, K.; Tsuchida, E. Catalytic Cycle of a Divanadium Complex with Salen Ligands in O2 Reduction: Two-Electron Redox Process of the Dinuclear Center (Salen = N,N′-Ethylenebis(Salicylideneamine)). *J. Am. Chem. Soc.* **1996**, *118* (50), 12665−12672.
(88) Oyaizu, K.; Yamamoto, K.; Yoneda, K.; Tsuchida, E. Multielectron Redox Process of Vanadium Complexes in Oxidation of Low-Coordinate Vanadium(III) to Oxovanadium(V) with Dioxygen. *Inorg. Chem.* **1996**, *35* (23), 6634−6635.
(89) Hills, A.; Hughes, D. L.; Leigh, G. J.; Sanders, J. R. Crystal and Molecular Structure of the Compound [(Salen) VOVO(Salen)][I5]·MeCN [Salen = N,N′-Ethylene-Bis(Salicylideneiminate)] and the Preparation of Similar Complexes with Other Schiff-Base Ligands. *J. Chem. Soc., Dalton Trans.* **1991**, *1*, 61−64.
(90) Thordarson, P. Determining Association Constants from Titration Experiments in Supramolecular Chemistry. *Chem. Soc. Rev.* **2011**, *40* (3), 1305−1323.
(91) Gutmann, V. Solvent Effects on the Reactivities of Organometallic Compounds. *Coord. Chem. Rev.* **1976**, *18* (2), 225−255.
(92) *Solvents and Solvent Effects in Organic Chemistry*, 1st ed.; John Wiley & Sons, Ltd, 2010. DOI: 10.1002/9783527632220.
(93) Gritzner, G. Solvent Effects on Redox Potentials: Studies in N-Methylformamide. *J. Electro. Chem. Interfac. Electrochem.* **1983**, *144* (1), 259−277.
(94) Gangi, D. A.; Durand, R. R. Binding of Carbon Dioxide to Cobalt and Nickel Tetra-Aza Macrocycles. *J. Chem. Soc., Chem. Commun.* **1986**, *9*, 697−699.
(95) Electrochemical Methods: Fundamentals and Applications, 2nd ed.; Wiley, 2000. https://www.wiley.com/en-us/Electrochemical+Methods%3A+Fundamentals+and+Applications%2C+2nd+Edition-p-9780471043720 (accessed 2022−08−11).
(96) Costes, J.-P.; Dahan, F.; Donnadieu, B.; Garcia-Tojal, J.; Laurent, J.-P. Versatility of the Nature of the Magnetic Gadolinium-(III)−Vanadium(IV) Interaction − Structure and Magnetic Properties of Two Heterobinuclear [Gd, V(O)] Complexes. *Eur. J. Inorg. Chem.* **2001**, *2001* (2), 363−365.
(97) Dutton, J. C.; Fallon, G. D.; Murray, K. S. Synthesis, Structure, ESR Spectra, and Redox Properties of (N,N'-Ethylenebis-(Thiosalicylideneaminato))Oxovanadium(IV) and of Related {S,N} Chelates of Vanadium(IV). *Inorg. Chem.* **1988**, *27* (1), 34−38.
(98) Fried, S. D.; Boxer, S. G. Measuring Electric Fields and Noncovalent Interactions Using the Vibrational Stark Effect. *Acc. Chem. Res.* **2015**, *48* (4), 998−1006.




https://doi.org/10.1021/acs.jpca.3c00827
*J. Phys. Chem. A* 2023, 127, 5324−5334